An Instrumented Glove for Grasp Specification in Virtual-Reality-Based Point-and-Direct Telerobotics

Myung Hwan Yun, David Cannon, Andris Freivalds, and Geb Thomas

***Abstract*— Hand posture and force, which define aspects of the way an object is grasped, are features of robotic manipulation. A means for specifying these grasping "flavors" has been developed that uses an instrumented glove equipped with joint and force sensors. The new grasp specification system will be used at the Pennsylvania State University (Penn State) in a Virtual Reality based Point-and-Direct (VR-PAD) robotics implementation. Here, an operator gives directives to a robot in the same natural way that human may direct another. Phrases such as "put that there" cause the robot to define a grasping strategy and motion strategy to complete the task on its own. In the VR-PAD concept, pointing is done using virtual tools such that an operator can appear to graphically grasp real items in live video. Rather than requiring full duplication of forces and kinesthetic movement throughout a task as is required in manual telemanipulation, hand posture and force are now specified only once. The grasp parameters then become object flavors. The robot maintains the specified force and hand posture flavors for an object throughout the task in handling the real workpiece or item of interest. In the Computer Integrated Manufacturing (CIM) Laboratory at Penn State, hand posture and force data were collected for manipulating bricks and other items that require varying amounts of force at multiple pressure points. The feasibility of measuring desired grasp characteristics was demonstrated for a modified Cyberglove impregnated with Force-Sensitive Resistor (FSR) (pressure sensors in the fingertips. A joint/force model relating the parameters of finger articulation and pressure to various lifting tasks was validated for the instrumented "wired" glove. Operators using such a modified glove may ultimately be able to configure robot grasping tasks in environments involving hazardous waste remediation, flexible manufacturing, space operations and other flexible robotics applications. In each case, the VR-PAD approach will finesse the computational and delay problems of real-time multiple-degree-of-freedom force feedback telemanipulation.**

I. Introduction

Point-and-Direct (PAD) robotics was initially explored by the second author at Stanford University [1]. This initial research demonstrated that an operator could direct a robot to perform tasks in a natural and interactive way by pointing to objects and destinations while giving directives such as "put that there" (Fig. 1). This point-and-direct approach was both an order of magnitude faster than teach pendant programming and less strenuous for a human operator than master-slave telemanipulation.

In demonstrations, this PAD Telerobot put trash in a wastebasket, and blocks on a pallet, and tools in a toolbox. These actions loosely represented tasks of hazardous waste disposal, manufacturing material handling, and space telerobotics. The Veterans Administration provided funding for development of the telerobot which was ultimately purchased in its entirety, including camera tower, mobile base, and articulated arm, by the NASA AMES Research Center in Sunnyvale, CA, for their mobile robotics activities.

Manuscript received April 23, 1994; revised August 29, 1996. This work was supported by the Ben Franklin Partnership Program of Pennsylvania under Project 92C.1054R-1.

M. H. Yun is with the Department of Industrial Engineering, Pohang University of Science and Technology, Pohang, Korea 790-784.

D. Cannon, A. Freivalds, and G. Thomas are with the Department of Industrial and Manufacturing Engineering, The Pennsylvania State University, University Park, PA 16802 USA (e-mail: axf@psu.edu).

Publisher Item Identifier S 1083-4419(97)05203-5.

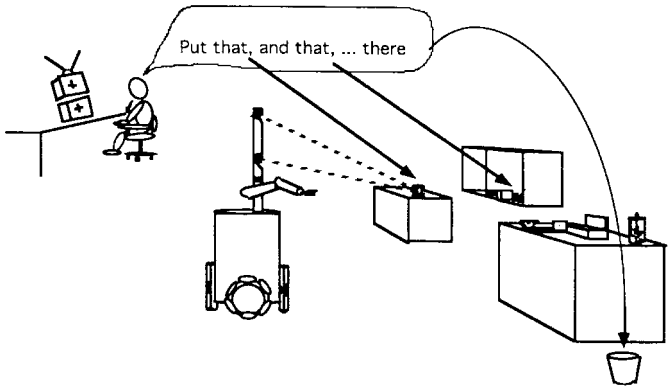

Fig. 1. To operate the Stanford PAD telerobot, a remote operator views two video monitors and aligns objects in each view by rotating the cameras on the robot much like remotely controlling a model airplane. After the operator points at each location, and gives directives as to what to do, the robot builds a task sequence and trajectory plan for its arm and mobile base to execute. The human strategically directs the robot at the object level in nearly real time. Before sending the robot to perform a task, or anytime during the task, the operator may review the proposed action for changes desired.

One limitation of the original Stanford PAD telerobot was that while it could be directed to pick up objects and release them at desired locations in unstructured environments, the orientation of the robotic gripper could not be easily specified. Because of this, the PAD telerobot was generally configured to approach objects along a line of sight proceeding to the target from where the robot was at the time of pointing.

Subsequent work in the Penn State VR-PAD Program has maintained the naturalness of pointing while providing orientation vectors as well as position coordinates using virtual tools that are interwoven into the live video scene. Such virtual tools, which are graphical representations of actual tools including robotic end-effectors, are simply flown to an object of interest in the scene by moving one's instrumented hand in free space (Fig. 2). This avoids laborious movement of a full multiple degree-of-freedom robot that has multiple links and often complex inertial dynamics. An invisible cut-plane, graphically draped at the object's depth, provides a correspondence between the virtual cyberspace in which graphics reside and the physical workspace in which real objects reside—so that virtual tools appear to engulf real objects in the interwoven reality scene. Solid rendering is changed to wireframe rendering behind the cut-plane. Once object and destination points are specified by engulfing an object, the robot calculates its own trajectories for moving from objects to destinations so the human need provide only task conception at the object level.

Thus, virtual tools have been interjected into a live videographic cyberspace creating an "interwoven reality" in which graphically represented end-effectors, such as a robot gripper, fly as if present in a real scene. Robots and machines can now be directed to do tasks in the same natural way that humans instruct one another using intuitive commands such as "put that there." Using this concept, the Penn State VR-PAD Program is developing an interactive system for hazardous material handling for Sandia National

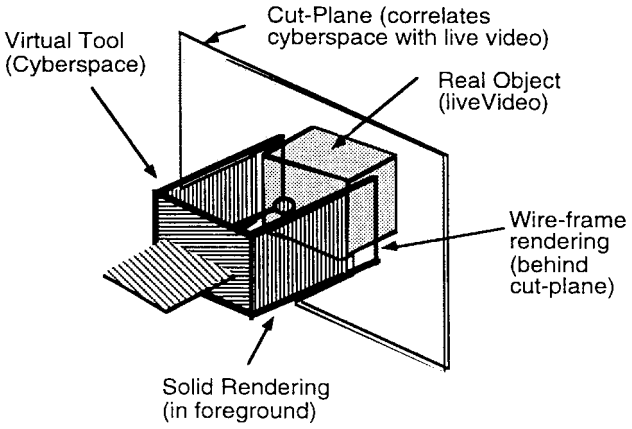

Fig. 2. A cut-plane, at a depth determined by camera triangulation, allows graphically represented robot end-effectors to fly in cyberspace and yet be correlated with objects in a live video scene. Thus, a virtual tool, such as the robot gripper shown, can be made to disappear behind a real object while a robotic task is specified at the object level.

Laboratories and for agile manufacturing for the National Science Foundation.

While previous to this work, the VR-PAD Program had successfully built a point-and-direct system with the basic features described above, the robot gripper of this implementation had always applied the same amount of force to every object and had no force feedback in the gripper fingers. There are cases in telerobotics, however, where robot hands have multiple fingers and where the magnitude of force must be specified. A heavy brick, for example, cannot be gripped in the same way and with the same amount of force as an egg because the thin wall of the egg will buckle under high loads. Yet, in developing a means of specifying variation in joint articulation and force, continuous full force feedback to the operator as in telemanipulation is not generally necessary. Specifying hand posture and force once for most objects is quite sufficient. (Even when reorientation is required *en route*, a simple algorithmic representation of dynamics in the presence of gravity may automatically adjust grasp force distributions without requiring human input). The human operator need not resort to manual control which may be time consuming, manually exhausting, and prone to unanticipated overshoot and error. Such telemanipulation is, after all, but one extreme on a telerobotics continuum that includes a potential line of possibilities stretching to full autonomy on the other extreme. The point-and-direct approach represents a class of telerobots sharing good characteristics of both extremes. VR-PAD interaction remains natural, and at the object level, while capabilities such as autonomous trajectory planning are fully utilized.

Toward the purpose of developing a simple means of specifying joint articulation and force at a point for a robot with sophisticated grasping capability, this study explores posture measurement and force sensing with Force-Sensitive Resistors (FSR's) implemented into an instrumented glove. Several observations about human grasping provide perspective. It is well known, for example, that humans heavily depend on force or pressure sensing when exercising a gripping action. As a person uses a tool such as a screwdriver, position and strain-sensing neurons in the muscle and tendon fibers of the hand, finger and wrist keep the brain informed about the overall spatial arrangement of the hand and the forces applied.

Many clues about the objects material properties—stiffness and strength—emerge from these senses. Specifically, a class of sensory neurons known as SA-I (slowly adapting system), which is arranged under the skin in a two dimensional grid like photoreceptors in a retina, gets credit as the primary means of perceiving, for example, the screwdriver's shape. This class of neurons also detects low-frequency vibrations that signal when the screwdriver has made contact with other surfaces, such as the groove on the head of a screw. A separate, denser grid of neurons—the rapidly adapting systems (RA)—relays spatial information, with about one third of the clarity of the SA system, but this grid can pinpoint much subtler movements between skin and surface, such as the vibrations that occur when a screwdriver slips slightly in the hand during turning. Such neural information presumably is the key to perceiving fine textures and adjusting the forces applied to tools during their use [2]. Approximating such tactile capability with artificial sensors is a challenge.

A practical approach to gripper control is suggested in this study while referencing the work of others including [3]–[6] who are similarly engaged. The approach presented here involves empirically based grasp specification and the use of a statistical model to preshape the gripper. Gripping control using an instrumented glove to provide joint/force coordination in virtual reality based point-and-direct robotics is explored. To specify hand posture and force distributions in a robotic gripper with two or more fingers, an understanding of the relationship between joint articulation and finger pressure must be acquired. An underlying model of this relationship is paramount. Instrumented gloves provide both an avenue to help understand the joint/force relationship and, later, an ideal input device to specify characteristics of grasping that will allow improved handling of an object without requiring manual control and robotic force feedback to the operator.

II. Background

The mouse-based click and drag approach of Apple Computer Company and others has been successful in a number of two-dimensional (2-D) on-screen computing applications. For three-dimensional (3-D) interaction, VPL Research was early in creating an instrumented glove that could be used to manipulate on-screen virtual images in an effectively 3-D graphical cyberspace. Their DataGlove system used optical fibers that measure the degree of bending of the user hand joints. A Polhemous magnetic sensor kept track of the absolute position of the hand with respect to a given source. The DataGlove has been used in various environments and was investigated by [7]. In an initial study, a resolution of better than 0.5° for an angle less than 36°, and better than 1.0° between 36° and 54° was obtained.

The Cyberglove, a similar instrumented glove, was chosen for this research. The tipless glove that allows fingertips to protrude was developed by Virtual Technologies Inc., Stanford, CA. The Cyberglove uses up to 22 strain gauge sensors: three bend sensors and one abduction sensor per finger, thumb and little finger [8]. In conjunction with the Cyberglove, a Pohlemeus magnetic sensor device (the same active locating element used with DataGlove) gives the position of the hand with respect to a reference. Both instrumented

gloves would be suitable for recognition of hand posture, and the use of an instrumented glove was found to be more effective than menu selections in a position and orientation speed test [9]. Furthermore, an instrumented glove can be modified with pressure sensors to differentiate the various gripping actions such as grasp, pinch, and firm grasp.

Many researches have been conducted to simulate the force control mechanism of the human hand. The control theory model is the most heavily mentioned approach (see [4]). As yet, however, there is no consensus regarding a universal idealization of a remote manipulator system. One ideal is to achieve a remote manipulator response that is a completely transparent interface between human and machine. In other words, the operator should feel as if the task object were being handled directly. Reference [10] suggests that the ideal telemanipulator can be represented by an infinitely stiff and weightless mechanical connection between the end-effector of the master arm and the slave arm. Reference [4] proposes a master–slave controller in which the human operator at the master port interacts with a task object at the slave port in a remote location. The gain of the force feedback was modeled to be selected based on the stability requirements and specification of the desired port impedance given models of the task and the human operator. Reference [11] proposes a model of bilateral control of force feedback and prediction. Mathematical modeling of a grasp function was conducted by [12]. They developed a mathematical model and an algorithm to plan the grasp action of a multi-fingered manipulator operating in uncertain environment. They divided the grip action into four steps; reach, preshape, enclose, and grip and developed separate algorithms to perform each step of the grasp phase for a multifingered robot hand.

Among experimental studies on remote manipulators, [5] performed an experiment for the remote manipulation tasks with various conditions of force feedback, direct viewing, visual angle, and task difficulty. Their result showed that the performance of the manipulation tasks with force feedback is the highest of all task combinations. Reference [3] developed a taxonomy of grasp function based on definition of power grip and precision grip in [13]. Using the taxonomy, he developed a scheme for selecting a particular grip posture for gripper manipulation. Reference [12] studied teleoperator comfort and psychometric stability by measuring finger forces and fatigue effects for the pinch forces of the human operators. Further, dynamics of the hand has been studied in the microsurgery environment. Reference [14] attached a force sensor and a location sensor on the operator hand and microsurgical tool and studied workspace and manipulation forces of a microsurgeon. In those applications, techniques of sensing force on the hand have also been considered important as well as in biomechanical studies and ergonomics. However, most techniques of sensing force exerted by human body segment have involved complex and expensive instrumentation with limited portability (see [15]–[18]). Moreover, there is a potential problem in applying the techniques to the measurement of hand force because of the relatively small size of the human hand and the high degree of irregularity of the surface of the hand. Nonetheless, recent technological advances have provided small, thin sensors with considerable promise for use in directly sensing individual finger forces during normal grasping activities. A conductive polymer sensor that can be attached to the palm surface of the hand is one such device [19]. Although somewhat limited in range and resolution, these sensors are highly durable and practical for measuring individual finger forces exerted during grip activity. A form of the same conductive polymer sensors, FSR's have recently begun to emerge as a major alternative. By using these latter devices, it was possible to measure the force distribution pattern of a hand tool, for example, during various activities [20].

FSR's are made from two sheets of polymer film (higher temperature polymide). On one sheet, a conducting pattern is deposited in the form of a set of interdigitating electrodes. Another sheet, with a proprietary semiconductive polymer film, is adhered across the finger network. Applying pressure to the matrix causes the resistance between the two contacts to decrease following an approximate power law [21]. Although the response to force changes is not linear, the FSR's can be calibrated for force measurement using a logarithmic regression [22]. The force/resistance response of an FSR is a sensitive function of the area being contacted. A typical FSR shows a response that varies as the reciprocal of the square root of the area of the applied force. The sensitivity of the FSR resistance to the area and distribution of the force shows that the FSR's must be used where the force footprint can be held constant in area, position, and distribution. The compliance of the force actuator (actual component or finger that physically contacts and transfers force to the FSR) affects the dynamic range of the FSR's. To overcome these difficulties in force measurement, plastic materials such as epoxy are usually overlaid over the FSR thus helping the device to concentrate the applied force. For a typical interface, the FSR is placed in series with a current source. The voltage measured across the FSR is then related to the applied force. A voltage is applied to the divider, and the output voltage, taken from the resistor/FSR junction, is measured. Transformation to digital data is advantageous for force measurement, since the log/log characteristic of the device can be translated to a linear relationship. In summary, the FSR is a simple and economical force sensor, compared to load cells and strain gauges. It is the smallest of the three sensors mentioned and can be attached to the human fingers without difficulty. With a proper mechanical arrangement of the constant contact force and distribution of each sensor, it is one the best sensor for measuring finger forces of the human hand.

III. Test Objectives and System Description

The basic motivation of this study is to acquire the data necessary for developing an efficient finger path planning method for the closing phase of grasping known as enclosure. The motion of a robot can be divided into five phases according to [6]: 1) reach phase; 2) preshape phase; 3) enclosure phase; 4) grip phase; and 5) manipulation phase. The performance of any grip action can be enhanced if precise information on the preshape, enclosure and grip phase are available before the initiation of the grip action. These, VR-PAD system with finger force input will provide using purely robotic force feedback.

Robotic systems can often determine an objects shape using machine vision based on a single picture, but force control generally requires continuous feedback information. [4] proposed an open loop force control system by predicting the force information ahead of

TABLE I
TASKS USED IN THE EXPERIMENT. THERE WERE EIGHT POWER GRIP TASKS, FIVE GRASP TASKS, AND FOUR PINCH TASKS. THE GRIP SIZE WAS MEASURED AS THE MAXIMUM DIAMETER OF THE TOOL WHERE THE HAND CONTACT IS MADE. IN CASE OF THE POWER GRIPS WHERE THE GRIP SHAPE IS NOT A CYLINDRICAL TYPE, THE GRIP SIZE WAS DEFINED AS THE MAXIMUM DISTANCE OF THE ENCLOSURE PROVIDED BY THE THUMB AND THE OPPOSING FINGERS

Grip Type	Tools used	Grip Size	Grip Shape	Simulated Task
Power Grip	Drill	4 cm	cylinder	drilling a hole
	Drill/w trigger	6 cm	cylinder	drilling a hole
	Knife	2.7 cm	shaped cylinder	cutting a carpet
	Hammer	3 cm	shaped cylinder	hammering a nail
	Hook	3.5 cm	square	pick up a piece of meat
	Screwdriver	7 cm	shaped cylinder	turn a screw
	Pliers	7.5 cm	shaped leg	grip a nut
	Scissors	6.5 cm	shaped hole	cutting a carpet
Grasp	Pulp grasp	N/A	cylinder	grasp a drum
	Medial grasp	N/A	cylinder	grasp a drum
	Mouse grasp	N/A	square	grasp a mouse
	Pen grasp	N/A	cylinder	grasp a pen
Pinch	Pulp pinch	N/A	N/A	pick up a plate
	Lateral pinch	N/A	N/A	pick up a plate
	Palm pinch	N/A	N/A	pick up a plate
	Finger press	N/A	N/A	press onto a surface

(N/A : not applicable)

signal feedback and then making the system gain "adjustable" based on the difference between modeled force and force feedback depending on the characteristics of a given task. In this research, a direct approach to force specification using force sensors impregnated into an operator's glove is explored where grasp information is transferred in the form of a specification to the autograsping manipulator based on finger pose and forces applied at the point of grasping using a surrogate object in the operator's hand. In this approach, the automatic feedback system simply maintains these specified forces during tool exertion so that the human need not provide continuous input to the manipulator. In our experiments to test this concept, the FSR's were attached to the human subject wearing an instrumented glove. Naturally, our FSR data may be useful to research in continuous telemanipulation as well.

It was hypothesized that the general tool grip postures of the human hand, as representative of a sophisticated robot gripper, can be described as a "quasigeneral" shape such that the control of the manipulator can be specified by an instrumented glove that provides an initial grip posture and related enclosure information to the manipulator. Based on these motivations, the objectives of the study were to:

1) measure finger articulation angles in grasping to determine initial measurements needed for specifying robotic grasp;
2) investigate the possibility of using FSR force sensors impregnated into an instrumented glove to specify the control of forces to be exerted on an object during grasping and manipulation;
3) measure the various force/position postures of the hand grasp function for an effective preshaped enclosure to test a model that can later be used with the VR-PAD telerobot developed at Penn State.

For the purpose of measuring the joint angles of the fingers and wrist joint, an angle transducer glove system (Cyberglove CG1801, [8]) and a set of data acquisition programs specific to finger joint measurement were developed. The Cyberglove system provided measurement of 18 joint angles. There were two flexion sensors on each of the five fingers. On the thumb, these two sensors measured the metacarpophalangeal (CMC) and interphalangeal (IP) joint flexions. On the remaining four fingers, the two flexion sensors measured the metacarpal phalangeal joint (MP) and proximal interphalangeal (PIP) joint flexions. Two wrist motions, flexion/extension and radial/ulna deviation angle, was also measured.

The hand calibration procedure included the joint location specification and the flexion calibration. First, the coordinate system of the hand based on the 3-D hand model by [23] was defined. Flexion-extension, radial-ulnar deviation, and axial rotation angles of the finger digits were also defined. The data from the Cyberglove, which represents the amount of finger movement expressed in the local coordinate system, was converted to the global coordinate system taking the wrist joint as the origin. The detailed description of the hand model used in this study can be found in [23].

The resulting joint flexion angles were digitized in radian format and transferred to a PC (Toshiba 3200). All of the hand calibration procedures were performed internally using the software program developed. The hand size and joint location of each subjects were measured prior to the experiment. The flexion sensor was calibrated individually using the hand model provided by the Cyberglove system.

For the measurement of finger forces, a sensor matrix with ten FSR's [21] was developed. This set up has been used to measure pressure distributions on foam grip handles [24], to study finger pinch forces [25], and hand tool coupling effects [26]. Each of the FSR sensors were covered with 2 mm plastic glue over a 12 mm^2 sensing area for effective force measurement. The sensors had a range of 1 to 50 N force with 1 N precision.

Voltage outputs from the ten sensors were recorded using a DASH 16/F analog-to-digital converter installed in a PC (Toshiba 3200). The glove was calibrated to force levels in Newtons (N) as a function of digitized voltage (V) value using a second order polynomial regression: $\text{Force}\,(\text{N}) = 0.23 - 0.61 * \text{voltage}\,(\text{V}) + 0.56 * \text{voltage2}\,(\text{V})$. The coefficient of determination for the pressure calibration regression was 0.98. The overall set up for the experiment is presented in Fig. 3.

TABLE II
THUMB FLEXION/ABDUCTION ANGLE. (AVERAGED ACROSS SUBJECTS IN DEGREES) AND WRIST FLEXION/DEVIATION ANGLE (AVERAGED ACROSS SUBJECTS IN DEGREES)

Task	CMC Flexion*	Abduction**	Wrist flexion***	Wrist deviation****
Screwdriver	5	-40	-15	-5
Finger press	-3	-40	-18	-8
Hammer	-25	-19	-7	-22
Hook	-30	-36	-12	-25
Knife	-19	-36	-8	-7
Lateral pinch	-15	-25	-5	-1
Medial grasp	-29	-23	-5	-12
Mouse grasp	-35	-27	1	-9
Palm pinch	-12	-25	-13	-3
Pen grasp	-16	-19	-18	-9
Pliers	-12	-9	-10	-9
Pulp grasp	-11	-23	12	-3
Pulp pinch	-46	-50	-22	-7
Power drill	-43	-51	-15	-3
Power drill (tr)#	-34	-34	-12	-10
Scissors	-31	-34	-22	-8

* For the thumb, (-) sign represents flexion, bending of the CMC joint. (+) sign represents the extension
** for abduction, (-) sign represents increasing the distance between the fingers (+) sign represents the fingers crossing each other.
*** for wrist flexion (-) sign represents flexion, bending of the wrist joint. (+) sign represents the extension
**** for wrist deviation (-) sign represents radial deviation (+) sign represents ulnar deviation
# Power drill (tr) Power drill tasks with trigger action

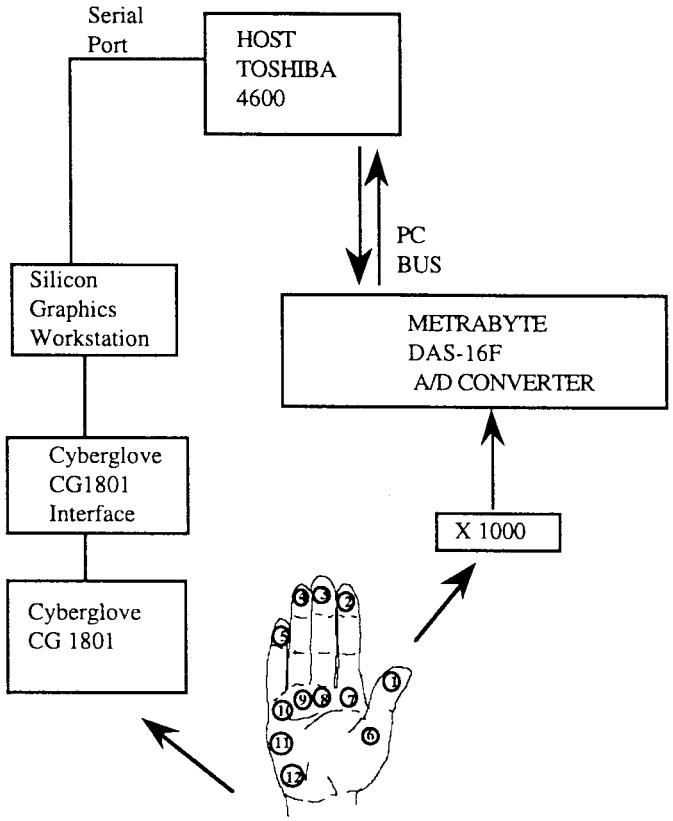

Fig. 3 Equipment was set up for the measurement. Joint articulation data was sent to separate interfaces and then transferred to a PC through a serial port. The force data simultaneously was recorded using an A/D converter. The number on the hand represents the location of the force sensors attached to the hand.

Fig. 4 shows the diagram of flexion angles and abduction angles measured by the Cyberglove system for the index finger. Positive sign was used for flexion angles and negative sign in the flexion angle specifies the corresponding extension of the joints. In abduction angles, positive signs were used to define ulnar deviation (twisting away from the thumb side) and negative signs were used for radial deviation (twisting to the side of the thumb).

In order to express a hand posture in a mathematical form, introduction of the three dimensional coordinate system is necessary. In this study, an individual 3-D Cartesian coordinate system was used at each joint of the finger as well as at the wrist joint. As shown in Fig. 4, the coordinate system of the wrist joint was defined as the origin point. The coordinate of each subsequent joint was defined with respect to the MCP joint (next to the wrist), PIP joint (second next to the wrist), and DIP joint (closest to the finger tip), respectively. At each joint, the proximal system (palm side) is related to the distal system (finger tip side) through a transformation. Eulerian angles are introduced to handle the transformation of the coordinates to the wrist origin. The reference position of each hand segment in this system is defined as zero degrees of articulation for all joints with respect to the proximal segments. Using an Eulerian angle transformation, proximal coordinates of a point defined at the distal coordinate system can be calculated [27].

The Z-Y-X Euler angle defined at any finger joint is

$$\begin{vmatrix} P'_x \\ P'_y \\ P'_z \end{vmatrix} = \begin{vmatrix} c\theta c\psi - s\psi s\phi s\theta & s\theta c\psi + s\psi s\theta c\phi & -s\psi c\phi \\ -c\phi s\theta & c\phi c\theta & s\phi \\ s\psi c\theta + c\psi s\theta s\phi & s\psi s\theta - c\psi s\phi c\theta & c\psi c\phi \end{vmatrix} \begin{bmatrix} P_x \\ P_y \\ P_z \end{bmatrix} \quad (1)$$

where

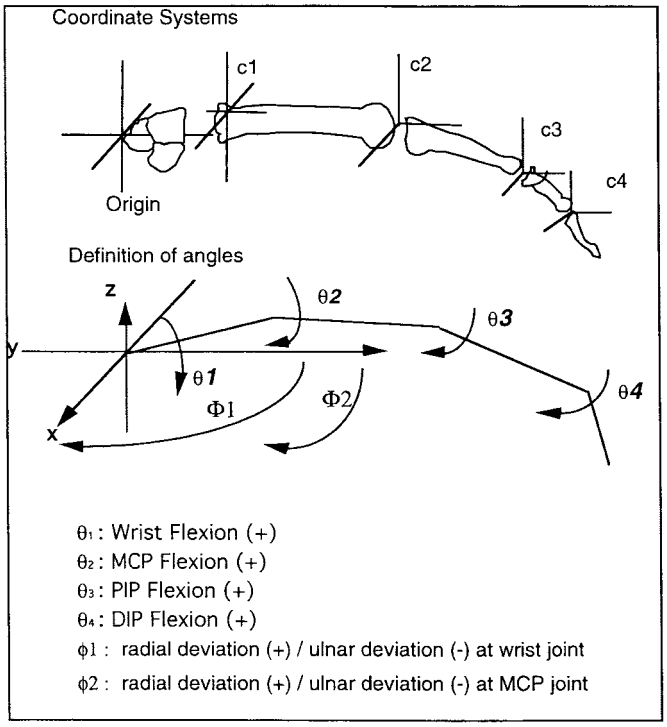

Fig. 4 The definition of the joint angles and the coordinate system of the hand; uses three dimensional Cartesian coordinate system at all of the hand joints including the wrist joint. Bending of the finger digits was represented by the flexion angles on the Y-Z plane and the deviation of the joints was represented by the deviation angles in the X-Y plane.

P'	parameters at the angulated posture;
P	parameters at the neutral posture;
c	cosine;
s	sine;
θ	flexion-extension angle;
ϕ	radial-ulnar deviation angle;
ψ	axial rotation angle.

If we consider the hand grip posture with no rotation, the Eulerian matrix becomes:

$$M = \begin{vmatrix} c\theta & s\theta & 0 \\ -c\phi s\theta & c\phi c\theta & s\phi \\ s\psi c\theta & -s\phi c\theta & c\phi \end{vmatrix}. \tag{2}$$

Therefore, the location of the joint i expressed in the $(i-1)$th coordinate is

$$\begin{vmatrix} X'_{i-1} \\ Y'_{i-1} \\ Z'_{i-1} \end{vmatrix} = [M_i]_{\phi i \theta i} \times \begin{vmatrix} X_{i-1} \\ Y_{i-1} \\ Z_{i-1} \end{vmatrix} + \begin{vmatrix} X_i \\ Y_i \\ Z_i \end{vmatrix} \tag{3}$$

where

X_i, Y_i, Z_i	coordinates of the ith joint;
$X_{i-1}, Y_{i-1}, Z_{i-1}$	coordinates of the ith joint defined at the coordinates of $i-1$th joint;
M_i	Euler matrix defined at ith joint;
θ	flexion-extension angle;
ϕ	radial-ulnar deviation angle.

Using (1)–(3), the algorithm to calculate the joint locations and force parameters on the hand during grasp action was defined. Based on the angle and force data from the measurement system, the program calculates the joint torques and moments at all joints of the hand.

A. Experimental Design

Six subjects were tested for 16 different hand tool tasks representing various types of human grasp activity and by extension the kinds of end-effector posture and force distributions that might be required of multifingered robots in the future.

The subjects were university students, all male, aged 23 to 29. Prior to the experiment, the subjects were measured for their hand sizes, finger digit lengths, and maximum grip strengths. There were eight grip tasks with cylindrical shapes and four precision grip (sphere shape) tasks as well as four pinch grip tasks. Subjects were initially asked to assume a hand position at zero flexion (a flat hand with the thumb attached to the index finger) for the recording of the reference point. They were, then, asked to grasp the tools as specified in Table I wearing the Cyberglove. The origin of the hand, the wrist joint, was fixed for all tasks. For the tasks with power grip with cylindrical shape handle (cases involving a drill, knife, hammer, hook, screwdriver, pair of pliers, and pair of scissors), FSR sensors were attached to the Cyberglove and the force data was measured simultaneously with the angle measurement.

For the angle measurement, the experimental design was a two-factor fully crossed factorial design with repeated measures. Both MCP flexion and PIP flexion angle were measured for the index, middle, ring, and little finger. One flexion angle (CMC joint flexion) was measured for the thumb. Five abduction angles from each finger were also measured as well as both wrist flexion and deviation angles. DIP joint angles were not measured from the sensor values since the flexion sensors were not attached to the finger tip area in the Cyberglove system. The Cyberglove system, however, estimates DIP flexion from the hand configuration model provided with the system. It was found from the preliminary experiment that the estimation of the DIP flexion from the Cyberglove system is accurate within $\pm 2^\circ$ using the mechanical goniometer as a reference. As studied by [13], DIP flexion is highly correlated with PIP flexion due to the fact that the tendons attached to distal and middle phalanges does not operate independent to each other. Hand force was measured at twelve different locations as seen in Fig. 3. Five sensors were attached to the finger tip area of the five fingers and the other five sensors were attached to the metacarpal area of the five fingers.

IV. Results and Discussion

A. Angle Measurement

The Analysis of Variance showed that both task ($F = 41.6, p < 0.01$) and fingers ($F = 522.9, P < 0.01$) had significant effect on joint angle as were the task*finger interaction. In Tables II and III, average joint flexion angle, finger abduction angle, and wrist flexion and deviation angle were summarized for the thumb and index finger for each task. Different tasks showed different patterns of angle for both the thumb and index finger. For most of the tasks in the experiment, the thumb was extended from 15–20°. Both pulp grasp and mouse grip tasks showed 10–15° more thumb flexion. For most power grip tasks (drill, knife, hammer, and hook), the MCP flexion ranged from 30–45° except the little finger that showed 10–15° less flexion.

Pinch tasks showed higher MCP flexion (i.e., indicating that this might be a good discriminating measure to look for when defining

TABLE III
FINGER FLEXION/ABDUCTION ANGLE (AVERAGED ACROSS SUBJECTS IN DEGREES) FOR THE INDEX, MIDDLE, RING, AND LITTLE FINGER

Tasks	Angles	Index	Mid.	Ring	Little	Tasks	Index	Mid.	Ring	Little
Knife	MCP flexion	23	35	49	60	Pulp	32	30	26	20
	PIP flexion	62	77	70	62	pinch	6	4	1	0
	Abduction	-6	0	6	10		-2	0	2	6
Hammer	MCP flexion	36	45	51	58	Lateral	40	40	39	41
	PIP flexion	64	68	57	44	pinch	61	73	71	73
	Abduction	-9	1	7	12		-3	0	3	7
Hook	MCP flexion	49	46	42	42	Palm	49	55	47	53
	PIP flexion	75	84	76	66	pinch	88	87	85	74
	Abduction	-8	0	9	16		-4	0	3	9
Pliers	MCP flexion	15	16	7	9	Finger	13	8	0	9
	PIP flexion	48	65	58	45	press	11	11	9	4
	Abduction	-6	1	5	15		-6	1	5	14
Screwdriver	MCP flexion	22	31	50	61	Pulp	21	26	22	24
	PIP flexion	57	71	62	53	grasp	37	34	26	16
	Abduction	-10	0	10	15		-4	0	4	15
Scissors	MCP flexion	19	12	15	17	Medial	10	19	15	10
	PIP flexion	63	58	52	47	grasp	47	40	34	31
	Abduction	-5	0	5	8		-7	1	5	16
Power	MCP flexion	26	28	18	16	Mouse	27	29	26	35
drill	PIP flexion	52	64	59	47	grasp	40	28	33	33
	Abduction	-10	0	10	15		-12	2	8	14
Power	MCP flexion	34	39	38	37	Pen	45	46	40	35
drill	PIP flexion	48	71	64	49	grasp	35	33	37	39
(trigger)	Abduction	-9	2	6	12		-4	1	3	7

pinching versus power grip tasks for a robot, for example). Both scissors and pliers grips showed 15–20° less flexion than the other power grips because of their extended grip postures. PIP flexion ranged from 50° to 80° for power grip tasks (drill, knife, hammer, and pliers). Pinch grips such as palm pinch, lateral pinch showed smaller PIP flexion from 30° to 40°. Comparison of the fingers from index to little finger showed similar flexion angles for power grips but significant difference between fingers for pinch grip tasks. This result supports the previous observation that the tools used with extended wrist posture such as knives, pliers, and scissors require a different grip posture than the other power grip tools.

A stepwise multiple regression was performed to estimate the joint angle from the hand anthropometry and tool grip size. The result of the regression is summarized in Table IV. The coefficient of determination, R^2, ranged from 62.4 to 86.6 for MCP flexion and 54.5 to 75.1 for PIP flexion.

It was found that the size estimates such as grip size, hand size, and digit lengths were good estimators of MCP angle but not as good when used as estimators to predict PIP flexion of a finger. It can also be postulated that the joint articulation of the grasp action can be defined from the human data except for the extreme cases where the physical hand size of the operator exceeds the normal range.

The plot of the finger flexion and abduction angle for the thumb and the index finger for the different grip sizes is presented in Figs. 5 and 6. The graph shows that the average MCP flexion decreased with increasing grip sizes. The increment of the flexion angles were most evident at the MCP joints and least evident at the DIP joints at the fingertips. For most grip sizes, the DIP joint angles were stable at about 40°. It can be postulated that the fingers exert their maximum gripping force with the DIP joints flexed at a constant angle regardless of grip sizes; and the fingers adjust themselves to different grip sizes mainly by changing the MCP and PIP joint angles.

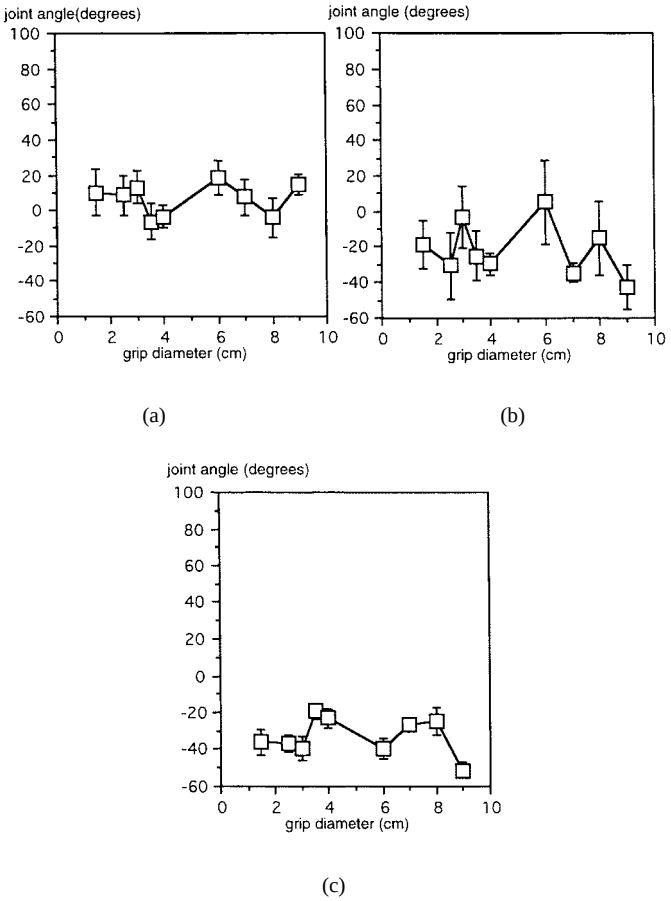

Fig. 5. Flexion angles of the thumb. The plot showed that thumb flexes does not show the effect of the diameter of the tools being grasped. It is likely that the thumb acts as a stationary base of the grip insensitive to size changes, and shows that thumb flexes more or less about the same amount in spite of increases in the diameter of the tools being grasped.

TABLE IV
RESULT OF THE REGRESSION ON JOINT FLEXIONS; THE MULTIPLE REGRESSION ANALYSIS SHOWED A SIGNIFICANTLY ($p < 0.01$) HIGH COEFFICIENT OF DETERMINATION (R^2) FOR ALL MODELS OF ESTIMATING JOINT ANGLES FROM SUBJECT DATA AND TASK TYPE

Finger	Joint	Const	Tool	GS	HL	HB	DL	MCP
II	MCP	94.1	—	-3.45	27.30	5.69	-61.02	
	(R^2=84.9)	(0.01)	—	(0.01)	(0.01)	(0.36)	(0.01)	
	PIP	138.4	—	-2.98	-3.78	—	—	—
	(R^2=54.5)	(0.01)	—	(0.01)	(0.01)	—	—	—
III	MCP	97.5	—	-4.1	34.83	-14.7	-62.1	—
	(R^2 = 62.4)	(0.05)	—	(0.01)	(0.04)	(0.01)	(0.07)	—
	PIP	95.22	—	-4.09	-6.17	12.12	—	—
	(R^2 = 53.8)	(0.02)	—	(0.01)	(0.01)	(0.01)	—	—
IV	MCP	221	-7.45	-4.97	-7.36	—	—	—
	(R^2 = 71.4)	(0.01)	(0.01)	(0.01)	(0.10)	—	—	—
	PIP	173.2	—	-7.44	—	—	-7.26	-0.49
	(R^2 = 62.7)	(0.01)	—	(0.01)	—	—	(0.04)	(0.01)
V	MCP	231	-2.46	-6.73	—	10.4	—	
	(R^2 = 69.8)	(0.01)	(0.02)	(0.01)	—	(0.12)	—	
	PIP	191	—	-9.09	35.1	—	-71.8	-0.52
	(R^2 = 75.1)	(0.01)	—	(0.01)	(0.03)	—	(0.01)	(0.01)

Where : TY : Tool type (0:power grip, 1:other grips with grip size), GR : Grip Size (cm), HL : Hand Length (cm), HB : Hand Breadth (cm), DL : Finger Length (cm), MCP : corresponding MCP flexion (Degrees), A,B...G : regression coefficient, εij : errors.

TABLE V
AVERAGE FINGER FORCES FOR EACH GRIP SIZES (N); TOOLS WITH CYLINDRICAL GRIPS WERE ANALYZED BY GRIP SIZE. NUMBERS IN THE PARENTHESIS ARE STANDARD DEVIATIONS FOR THE AVERAGE FORCE

	Grip Diameter	Hammer 3 cm	Power Drill 4 cm	Scissors 6.5 cm	Screwdriver 7 cm	Pliers 7.5 cm
Thumb	DIP	13.2	3.7	20.0	19.4	33.0
		(8.6)	(2.7)	(12.1)	(11.8)	(10.2)
	MP	10.9	18.0	9.0	7.4	1.9
		(5.1)	(7.4)	(6.2)	(4.0)	(1.9)
Index	DIP	19.9	44.0	17.0	17.7	37.4
		(11.9)	(12.3)	(11.8)	(15.0)	(19.2)
	MP	9.9	37.6	15.0	15.3	2.2
		(4.9)	(25.0)	(5.2)	(9.3)	(2.3)
Middle	DIP	6.1	28.4	17.7	19.2	13.0
		(2.0)	(11.9)	(12.0)	(11.8)	(12.0)
	MP	7.8	10.3	17.7	24.6	2.2
		(2.0)	(4.0)	(12.2)	(5.0)	(2.3)
Ring	DIP	20.5	31.5	20.3	31.0	19.0
		(12.0)	(12.1)	(11.8)	(21.6)	(7.4)
	MP	9.1	5.6	2.1	3.1	2.2
		(4.3)	(2.1)	(2.1)	(1.2)	(2.3)
Little	DIP	19.6	7.9	6.0	4.6	10.9
		(9.3)	(6.5)	(2.1)	(5.7)	(11.6)
	MP	1.4	0.8	1.8	2.1	1.3
		(2.2)	(2.1)	(2.2)	(2.2)	(2.2)

In other words, the grasp action can be explained as a sequential movement from the wrist side to the finger tip side. It seems that the major flexion of the first joint from the wrist is performed first for the rough sizing of the grasp area. Then, the next joint (PIP joint) was involved in a tighter, and more precise grasping of the object being handled. And, finally, the finger tip movement (DIP joint) is primarily configured for the enclosure and, for some part, force exertion. Sensing these joints in particular would provide us with the information needed to direct a robot to perform a similar grasp geometry on a remote object. As will be seen, this information plus force on the tip of the thumb and a single digit (the index finger) will be sufficient to calculate both pose and finger pressure requirements for many cases.

The abduction angles were stable at $10^\circ \pm 2^\circ$ for most grip sizes from the index finger to the little finger. It seemed that the grip force was maximized when the fingers were spread by 10° to the

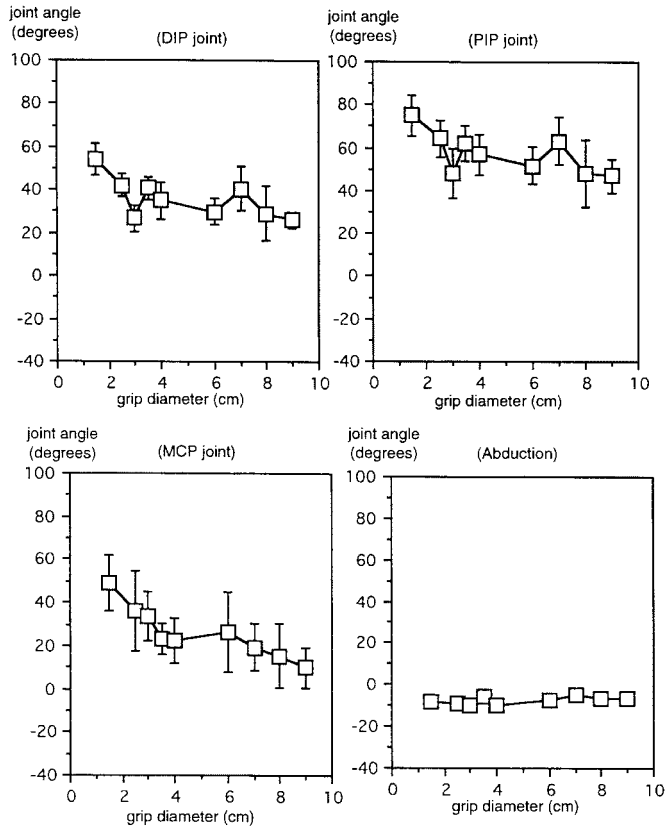

Fig. 6. Flexion angles of the index finger shows that flexion angles decreases as grip diameter increases. Abduction angle shows a very little change for all test conditions.

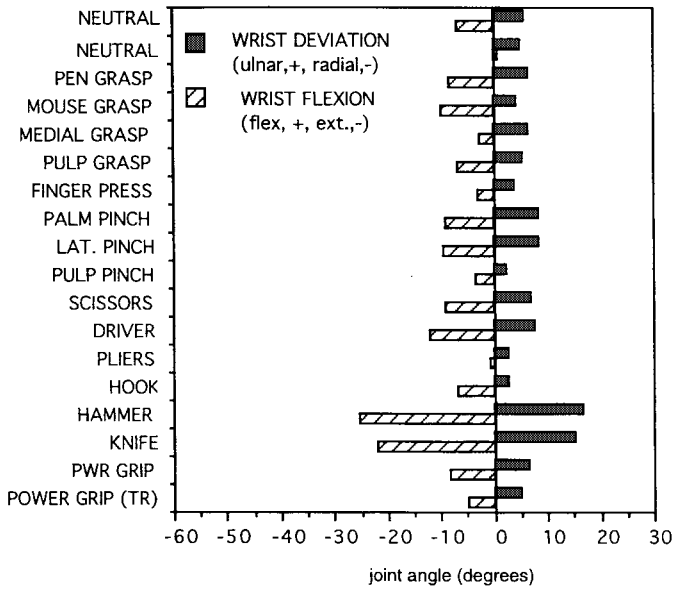

Fig. 7. Wrist flexion and deviation angles by task types shows that hammer and knife grip tasks involve different angles than the rest of the grip tasks. More flexion and deviation was noticed in those grip tasks compared to other tasks where the wrist angle showed 10° flexion for the maximum grip. More wrist flexion was noticed for the tasks with precision grip and fast action of the hand.

grip shape except in the case of very small objects where increasing the abduction angle is not possible without dropping the object. The average wrist deviation angles, both flexion/extension and radial/ulnar deviation, is shown in Fig. 7.

For most tasks, the wrist was extended around 10° ±3° except for the hammer and knife grips where the wrist was extended 20° to 25°. The wrist extension can be used as an indication of the characteristics of a grip. "Diagonal volar grasp" [28] with the wrist extended is advantageous for precise movement and "transverse volar grasp" with the wrist flexed seemed to be used for effective force exertion.

Based on these results, the grasp specification can be defined based on the grip size of the object and a human dimension related to hand size. The general grasp specification can be generated from the hand model. Grasp geometry, therefore, could be specified by monitoring glove joint articulation sensing in the glove without requiring extensive force feedback and visual aids on a continuous basis from the remote environment.

B. Force Measurement

In the two-factor ANOVA, the finger force was significantly different between the tools ($F = 217.9,\ p < 0.001$) and digits ($F = 94.4,\ p < 0.01$). Both the thumb and index finger force were significantly different while the middle, ring and little finger showed no significant difference ($p > 0.1$). Average value for the sum of all five finger forces was 168 N (s.d. = 20). This value was lower than the value reported by [25] where the average force was 183 N (s.d. = 15) for static pinch grip posture. Table V shows the average force level and standard deviations for each finger for the five different grip sizes.

The effect of the finger forces due to different grip size is represented graphically in Fig. 8.

In general, the finger tip area (DIP joint) was the site of greater force compared to the metacarpal area for all grip sizes. The result also supports the observation that the forces acting on the tool is mainly controlled by the finger tip area rather than the force acting on the other joints. The thumb seemed to work primarily as a stationary base against which grasping takes place with the opposing force of the fingers presumed to be situated at the base of the thumb (Fig. 9).

The contribution of each finger to the total grip force is presented in the Fig. 10. The thumb and the index finger contributed a large portion of the grip force for the tools with bigger grip sizes and showed lesser proportional contribution in smaller grip sizes. It can be assumed from the result that the two finger motion, the thumb and the index, is the source of the grasp power for the grasp types of cylindrical shape. Other fingers showed a support function mainly maintaining the grasp posture itself. Similar results have been argued in [29] where they tested the pinch type grasp action. Finger tip area showed an increased force level as the grip size increased while the force acting on the metacarpal area showed a decreased contribution as the grip size increased.

Overall, it was found that the grip force is a complex function of the size of the object, shape of the contact surface, and the types of the tools used. However, it was found that finger forces, index finger in particular, can be measured and used for specifying the amount of force needed to maintain the grasp posture of the hand. Together with the joint angle data of the hand at that specific posture, a good designation of position and force requirements could

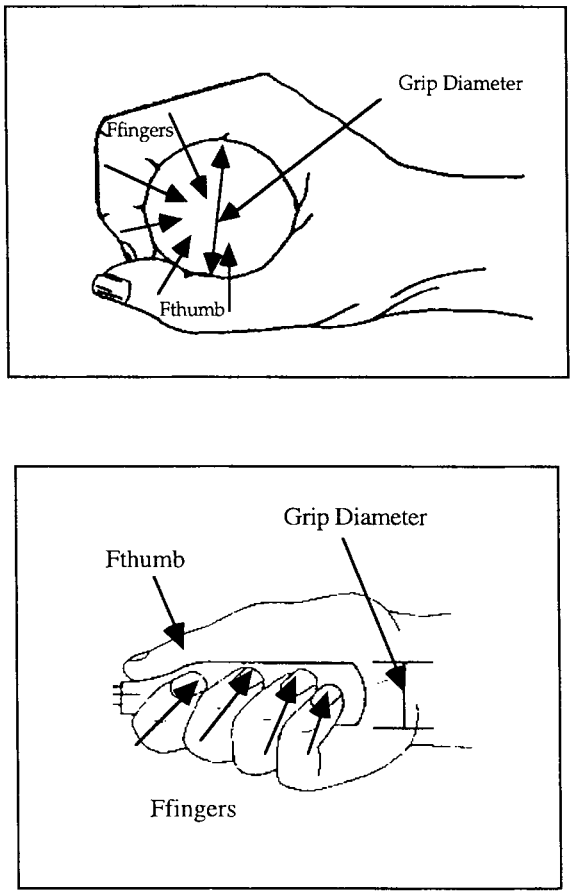

Fig. 8. Finger forces by grip diameter show that the thumb tip force increases as the grip diameter increases. The index finger force show minimal change due to grip diameter as well as the middle finger force. However, force from the base of the middle finger increased significantly as the grip diameter become larger. Little finger force decreased as the grip diameter increases.

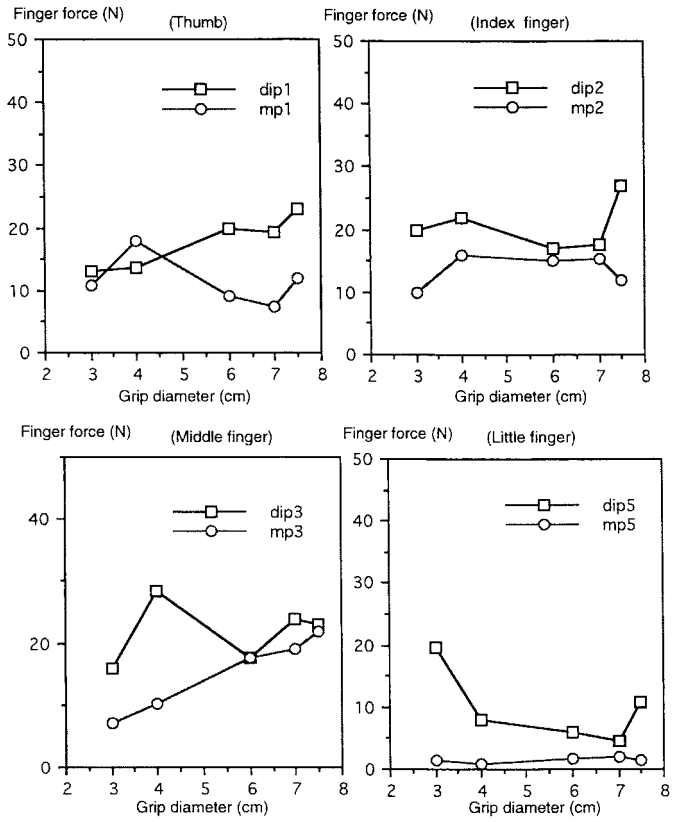

Fig. 9. Opposing force generated from the thumb is divided into two components. Force from the opposing thumb tips used to control the tool as shown in the figure while the base fingers provide the reaction force.

be possible for a robot. The force specification, is presumed to be initiated from the human operator based on his or her knowledge of the objects being grasped. The human operator holds an object similar to the one in the remote environment such as a brick. With the measurement system developed in this study, hand and finger posture as well as force to be applied are then relayed to the robot based on grasping performance using the instrumented glove. The force and position sensors attached to the Cyberglove system recognize the posture and the amount of force exerted to the finger tips and transfer the data as a specification to the manipulator for it to maintain during an otherwise autonomous grasping endeavor. With a basic robot algorithm to adjust for movement with gravity and to increase forces with the onset of slip, the instrumented glove specification system should allow the human to provide important data yet operate at a much higher level of strategic control than is possible with continuous telemanipulation. Again, if desired, the instrumentation derived for our purpose could also be applied to the continuous telemanipulation case provided data is acquired and perceived in the real time.

C. Force Control

The common purpose of force control during the preshape phase of grasping is to allow forces to be gradually applied to preshape the hand into a configuration with grasping pressure suitable for the anticipated action. Our data here is focused on the "prehensibility" in which joint articulation data is used in conjunction with a visual aid to determine hand shapes from a list of object types and object properties and high-level task specifications. Objects can be described based on size (grip size, volume), geometry (i.e., cylindrical), topology (e.g., number of vertices, edges, faces), and functionality (e.g., tool function). Fig. 11 shows a typical time curve for the force values of the five fingers when an operator lifts a square object. As seen in the figures, there is an initial overestimation of the forces from the finger tip at the initial stage of the lift. The force value is then stabilized over time as the operator adjusts his/her grip force to the amount needed to maintain the gripping action. It seemed from the test that the force values of the fingers were critically balanced to maintain the forces necessary to lift the brick. It is the stabilized value that must be specified for the robot to execute the task (provided additional forces necessary to lift the arm and the gripper are maintained).

The stabilization phenomenon in Fig. 10 can be seen by the several adjustments of the forces between the fingers over time particularly in the first half second. Our results also show that the grip forces from the FSR sensors follow a general pattern over time. The typical time curve for the forces could, in fact, be programmed to control the manipulator if robot grasping is to fully mimic human grasping. Alternatively, the robot could be allowed to perform superior grasping transition based on similar or better finger force adaptation to attain

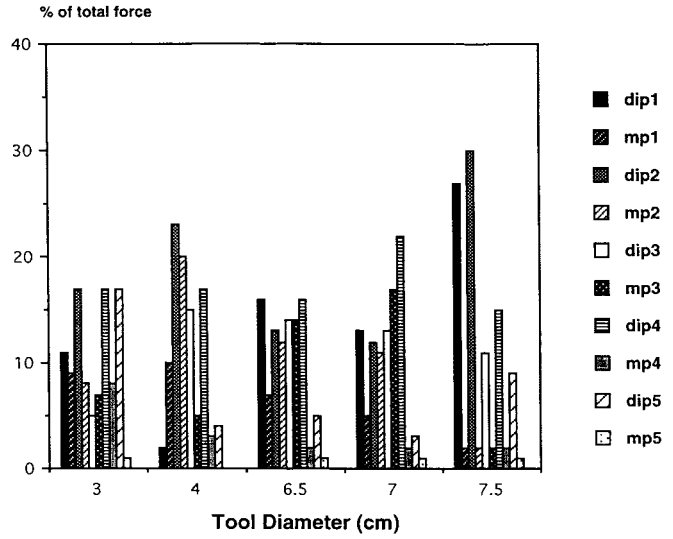

Fig. 10. Percentages of the total force for all fingers by grip diameter shows that the proportion of the thumb and index finger increased as the grip diameter was increased. The higher the requirement of the grip diameter, more of the thumb and index finger action provided most of the force while the other fingers provided only a supporting function on the grip part of the task.

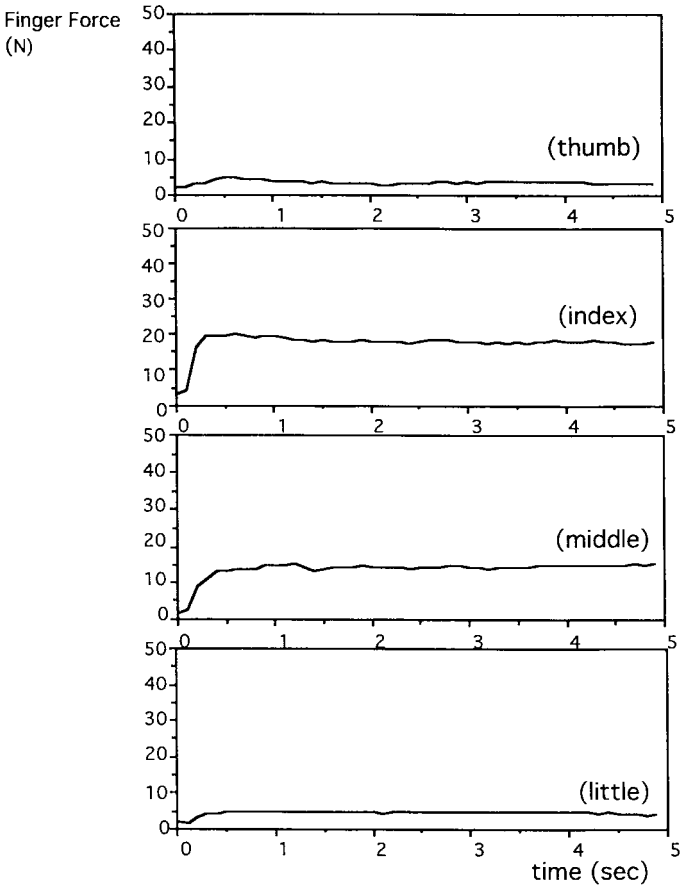

Fig. 11. Time curves of the finger forces when lifting a square brick show that some adjustment in forces initially takes place until a stable grasp is established.

the required force levels if controllers are implemented that overcome human limitations such as neuromuscular lag and reaction time delays. In any case, human fatigue will be significantly improved in the point-and direct approach.

At the enclosure phase during which the object is being completely enclosed within the grasping fingers, it is necessary to have the data on the preshaped hand and the desired Cartesian location of the finger joints.

A 3-D hand model using the coordinate system presented in the system description section and the joint location data provided in [23] was developed. The result of the hand model includes the location of finger tips and each joint of the hand as well as the torque and moments generated at the finger joints due to external forces. The model can be used to monitor the torques and moments of the gripper generated at the joints in a specific grip posture during autograsping. As an initial validation, a calculation of the vertical component of forces and moments generated at the finger joints using the force data developed in this study was conducted. The procedure used a 3-D biomechanical model of the hand with Eulerian angle transformation adapted from [23]. A software program routine was also written to implement the procedures and interface them to the grasp specification systems developed.

Our own test results from this model including index finger joint forces and moments transformed to the normalized force value (the ratio of the unit force), was compared with the results for the index finger obtained by [23]. The resulting vertical joint torques and moments of the index finger for this task ranged from 0.03 to 1.92 times the unit force applied for the PIP joints and 0.13 to 1.35 times the unit force for the MP joints. Both results were well within the range published in [23] which has a much wider value range.

Finally, the force measurement system can assess finger forces on the object in the grasp phase. As the object is grasped, the actual force can be deduced from the finger forces sensed on the operator. This information can be transferred to the manipulator as an indication of the external forces to be applied by the gripping fingers to the real object in the remote workspace. Using the index finger sensor only, the model is able to calculate other finger forces based on hand geometry to within the standard error of the regression equation (in our model, it was about 5%).

Limitations to be considered in applying these results include several discussion points. First, for all testing, the instrumented glove was worn on the left hand (designed to allow the right hand to remain free for mouse and key stroke activities in our application). While a majority of operator's will have previously operated tools in a right handed manner, the effect of using the left hand instead of the right is unknown. No noticeable incoordination was observed during testing, however. Second, the experimental results presented here are from tracking the human hand. While a multi-fingered manipulator may benefit from these human hand results in future grasp models, it is not clear at this stage whether all aspects of current testing will transfer exactly to the case of much simpler grippers of basic parallel jaw configuration. It can be postulated, however, that the thumb and the index finger model can be used for the two-jaw gripper since the experimental result showed that most of the grip action is controlled by the action of the thumb and the index finger provided the base of the thumb and other fingers are approximated and accounted for in designating forces on gripper jaw pressure.

V. Conclusion and Future Research

In a grasping that is specified using an instrumented glove, both flexion angles and finger forces were found to vary for the fingers engaged in different grip tasks. Control of the joint angle changes for the different grip sizes seemed to be achieved primarily by the changes in the MCP angle on the first joint of each finger.

The gripping process was observed to be a sequential flexion of finger joints from the proximal side to the distal side of the hand. The experimental results agreed well with the original expectations with regard to the ranges of joint articulation and the forces acting on the fingers. For example, the typical grip angle was around 40° around the DIP joints, 60° to 80° around the PIP joints, and 20° to 40° for MCP joints.

The result of force analysis for the different grip sizes showed that main force exertion is executed by the thumb and the index finger while the other fingers showed a supporting and calculatable role during most of the tasks in the experiment. This suggests the possibility that reduced FSR placement on only the thumb and the tip of the index finger might be sufficient if a reliable relationship between these two and the other fingers can be quantitatively established for the cases effected. This support role pattern for the minor fingers was most distinctive when the grip size was large. Most importantly, the results suggest that the hand anthropometry and task characteristics such as grip span and grip type can be used to estimate the hand MCP flexion and PIP flexion and therefore could be used to specify grasp requirements for a robotic end-effector.

These results suggest that use of these primary parameters to specify robot grasping will aid the grasp phase including the designation of posture and force in telerobotics control. This simultaneous specification of force and joint articulation serves as a first step toward improving human supervision of grasping for remote telerobotics particularly in the case where humans point and give directions rather than provide continuous telemanipulative input. The robotics community may progress further toward such strategic control of grasping as more sophisticated robot mechanisms are developed. With such robotic capability adapted to the point-and-direct paradigm, the role of the human may be raised to the level of giving target grasping angles and forces while letting the robot adjust and maintain a reliable grasp during its own complex trajections. Future research may consider the proper means to specify articulation angles and forces for robot grippers even when these grippers do not exactly resemble the human hand or the instrumented glove used to develop the grasp specifications. Future research may also use the ability to sense the onset of frictional slip during grasping and another capabilities as they become technologically possible.

References

[1] D. J. Cannon, *Point-and-Direct Telerobotics: Object Level Strategic Supervisory Control in Unstructured Interactive Human-Machine System Environments*, Stanford University, Stanford, CA, Ph.D. dissertation, (available from UMI Dissertation Information Service, Ann Arbor, MI), 1992.

[2] C. G. Philips, *Movements of the Hand*. Liverpool, U.K.: Liverpool Univ. Press, 1990.

[3] R. D. Howe, "Human grasp choice and robotic grasp analysis," in *Dextrous Robot Hand*, S. T. Venkataraman and T. Ibreall, Eds. New York: Springer-Verlag, 1990, pp. 5–21.

[4] T. B. Sheridan, G. J. Raju, F. T. Buzan, W. Yared, and J. J. Park, "Adjustable impedance, force feedback and command language aids for telerobotics," in *Proc. IEEE Conf. Systems, Man, Cybernetics*, 1991, vol. IV, pp. 81–88.

[5] C. L. Mackenzie and T. Iberall, *The Grasping Hand*. New York: North-Holland, 1994.

[6] A. M. Erkmen and H. E. Stephanou, "Grasp planning under uncertainty," in *Proc. IEEE Conf. Systems, Man, Cybernetics*, 1991, vol. IV, pp. 447–456.

[7] E. R. Tello, "Between man and machine," *BYTE*, Sept. 1988.

[8] Virtual Technologies, *CyberGlove*™ *System Documentation*, Virtual Technologies, Palo Alto, CA, 1992.

[9] D. J. Cannon, G. Thomas, C. Wang, and T. Kesavadas, "A virtual reality based point-and-direct robotic system with instrumented glove," *Int. J. Ind. Engineers—Applicat. Practice*, vol. 1, no. 2, pp. 139–148, 1994.

[10] M. Handllykken and T. Turner, "Control system analysis and synthesis for a six DOF universal," in *Proc. IEEE Int. Conf. Robotics Automation*, 1986, pp. 1520–1532.

[11] R. J. Andersson and M. W. Spong, "Bilateral control of teleoperators with time delay," *IEEE Trans. Automat. Contr.*, vol. 34, no. 5, pp. 494–501, 1989.

[12] S. F. Wiker, E. Hershkowitz, and J. Zik, "Teleoperator comfort and psychometric stability: Criteria for limiting master-controller forces of operation and feedback during telemanipulation," in *Proc. IEEE Conf. Systems, Man, Cybernetics*, 1991, vol. IV, pp. 99–107.

[13] J. R. Napier, *The Hands*. New York: Pantheon, 1980.

[14] S. Charles and R. Williams, "Measurement of hand dynamics in a microsurgery environment: Preliminary data in the design of a bimanual telemicro-operation test bed," in *Proc. IEEE Conf. Systems, Man, Cybernetics*, 1991, vol. IV, pp. 109–118.

[15] R. P. Betts, C. I. Franks, T. Duckworth, and J. Burke, "Static and dynamic foot pressure measurement in clinical orthopedic," *Med. Biolog. Eng. Comput.*, vol. 18, pp. 674–684, 1980.

[16] R. W. Soames, C. D. Blake, J. R. R. Scott, A. Goodbody, and D. A. Brewerton, "Measurement of pressure under foot during function," *Medica. Biolog. Eng. Comp.*, vol. 20, pp. 489–495, 1979.

[17] E. M. Henning, P. R. Cavanaugh, H. T. Albert, and N. H. McMillan, "A piezoelectric method of measuring the vertical contact stress beneath the human foot," *J. Biomed. Eng.*, vol. 4, pp. 213–222, 1982.

[18] T. E. Treaster and W. S. Marras, "Seat pressure: Measurement and analysis," *SAE Tech. Paper Series*, no. 890849, 1989.

[19] T. R. Jensen, R. G. Radwin, and T. G. Webster, "A conductive polymer sensor for measuring external finger forces," *J. Biomech.*, vol. 24, pp. 851–858, 1991.

[20] M. H. Yun, "Development of hand posture measurement system to evaluate manual tool tasks," in *Proc. Human Factors Ergonomics Soc.*, Seattle, WA, 1993.

[21] Interlink Electronics, *FSR: Force and Position Sensing Resistors*, Santa Barbara, CA, 1989.

[22] K. T. Stone and C. L. Vaughan, "A new transducer Technology for measurement of plantar pressures," in *Biomechanics XII*, Los Angeles, CA, abstr. 100, 1990.

[23] E. Y. S. Chao, K. N. An, W. P. Cooney, and R. L. Linscheid, *Biomechanics of the Hand—A Basic Research Study*. Singapore: World Scientific, 1989.

[24] G. L. Fellows and A. Freivalds, "Ergonomic evaluation of a foam rubber grip for tool handles," *Appl. Ergonomics*, vol. 22, no. 4, pp. 225–230, 1991.

[25] R. G. Radwin, S. Oh, T. R. Jensen, and T. G. Webster, "External finger forces in submaximal five finger static pinch prehension," *Ergonomics*, vol. 35, no. 3, pp. 275–288, 1992.

[26] R. Bishu, W. Wang, and A. Chin, "Force distribution at container handle-hand interface," *Appl. Ergonomics*, vol. 11, no. 3, 1993.

[27] J. J. Craig, *Introduction to Robotics*. Reading, MA: Addison-Wesley, 1988.

[28] B. O. Buchholtz, "A kinematic model of the human hand to evaluate its prehensile capabilities," Ph.D. Dissertation, Univ. Michigan, Ann Arbor, 1989.

[29] G. Westling and R. S. Johansson, "Factors influencing the force control during precision grip," *Exper. Brain Res.*, vol. 53, pp. 277–284, 1984.